Automated Assessment of the Curliness of Collagen Fiber in Breast Cancer

Anonymous ECCV submission

Anonymous Organization

Abstract. The growth and spread of breast cancer tumor are influenced by the composition and structural properties of collagen in the extracellular matrix of tumors. Straight alignment of collagen has been attributed to tumor cell migration, which is correlated with tumor progression and metastasis in breast cancer. Thus, there is a need to characterize collagen alignment to study its value as a prognostic biomarker. We present a framework to characterize the curliness of collagen fibers in breast cancer images from DUET (DUal-mode Emission and Transmission) studies on hematoxylin and eosin (H&E) stained tissue samples. Our novel approach highlights the characteristic fiber gradients using a standard ridge detection method before feeding into the convolutional neural network. Experiments were performed on patches of breast cancer images containing straight or curly collagen. The proposed approach outperforms in terms of area under the curve against transfer learning methods trained directly on the original patches. We also explore a feature fusion strategy to combine feature representations of both the original patches and their ridge filter responses.

Keywords: Collagen, Deep Learning, Ridge Detection, Digital Pathology

1 Introduction

Collagen is an abundant structural protein in the extracellular matrix of tissues. In addition to providing structural support, collagen also plays a major regulatory role in other tissue functions, including cell adhesion, migration, and proliferation. Recent experimental and clinical studies have shown how the structural integrity of collagen directly influences the behavior of breast cancer (BCa) cells and their capacity for metastasis.

Compelling evidence has emerged to show how the structure and alignment of collagen is correlated with BCa progression and metastasis. Our goal is to use deep learning to characterize these architectural features by classifying whether collagen appears straight or curly in BCa images. Therefore, we utilized the DUET imaging technique (DUal-mode Emission and Transmission) [11], which focuses on color (spectral) differences in H&E fluorescence to directly highlight collagen distributions in H&E slides. Compared to existing techniques, DUET uses readily available H&E slides with the potential to be a better collagen detection tool in clinical settings due to low cost, simplicity, rapid imaging speed,

and non-destructive effects in tissue samples. See Fig. 1 for examples. Quantitative methods to identify collagen structure orientation patterns in DUET images have not been explored.

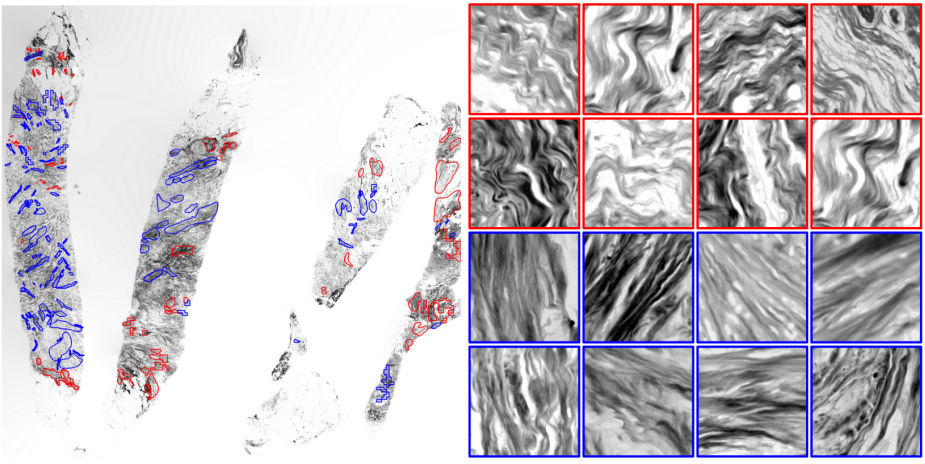

Fig. 1. Example DUET images capturing different collagen fiber patterns. Left: red and blue contours highlight regions of interest (ROIs). Preliminary annotations are given to these ROIs. Red circles enclose regions which are dominantly curly. Blue circles enclose regions which are dominantly straight. Right: Patches were sampled from these ROIs and are individually annotated by expert annotators. Red boxes enclose curly patches and blue boxes enclose straight patches. Annotations of individual patches are correlated to but are not fully consistent with the annotations of ROIs. For example, a dominantly curly region may contain straight patches.

We present a deep-learning-based automatic method to classify BCa DUET image patches into two categories, curly and straight, based on given annotations by our domain expert (Fig. 1). There are two challenges for the direct application of deep neural networks: First, the amount of training data is relatively limited. It is insufficient for training a deep neural network classifier from scratch. Second, the distinct geometry and textural patterns of collagen fiber patches makes it hard to directly use neural networks trained on other pathology images (mostly H&E). On the other hand, classic image filters are well designed to characterize object flow and detect these collagen fiber structures of interests.

Our novel approach combines the strengths of both deep neural networks and classic image filters. In particular, we leverage classic second-order-derivatives-based filters that are well-designed for identification of collagen fiber structures. The identified structures are combined with deep neural nets pretrained on public datasets for the best classification of curly vs. straight fiber patterns. We also explore different existing approaches for feature fusion in order to find the best strategy for our application. Usage of the classic filters that are well-suited

to the structure of interest alleviates the demand of training data from deep networks. Meanwhile, incorporating these filters with pretrained deep nets ensures the structural features can be fully leveraged in a data-driven manner. Inspired by the analogy of the collagen images with "flow" images and the use of second-order derivative filters for optical flow computation, we experiment with two stream networks analogous to those successfully applied in video analysis tasks, where spatial (frames) and temporal information (optical flow) are aggregated [30,26,10].

In summary, our main contributions are:

1. We present the first deep learning approach to capture orientation patterns of collagen fibers;
2. We incorporate sophisticated image filters (i.e., ridge detectors) that are very appropriate for highlighting fiber structures in a two-stream deep learning framework.
3. We evaluate our methods on a unique cohort of DUET collagen images. We demonstrate that incorporating these additional structural features will significantly improve the generalization performance of the classifier, especially when there is insufficient training data.

2 Background

Importance of Collagen in Breast Cancer: Brabrand et al. [1] studied the structure of collagen fibers in intratumoral, juxtatumoral, and extratumoral regions and classified collagen fibers as (1) curly or straight and (2) parallel or not parallel. They observed that collagen fibers appeared more straight and aligned at tumor boundaries while tumor cells invade surrounding tissues. In another study, Carpino et al. [3] observed correlations between the reorganization of collagen and progression. Early in tumorigenesis and during the initial stages of tumor progression, collagen appears to be mostly curly and dense. As tumorigenesis progresses, collagen architecture becomes straight and aligned in parallel to the tumor boundary. In more advanced stages of tumor progression, collagen fibers are oriented perpendicular to the tumor boundary. These and other studies indicate that the structure and alignment of collagen in close proximity of BCa can be a critical indicator of tumor progression [27,28,4,31,6].

The association between collagen alignment with breast tumor progression and metastasis underlies the need for quantitative methods to extract and characterize useful information from collagen-tumor relationships. A variety of techniques have been proposed to capture images of collagen fibers in tissue specimens [24,8,2,7]. Collagen fiber orientation may be quantified using Spatial Light Interference Microscopy (SLIM). Majeed et. al. [20] have used SLIM images to extract prognostic information from BCa collagen fibers. Second harmonic generation (SHG) microscopy techniques have been used to localize patterns associated with collagen fiber extracellular matrix without the need for specialized stains. Collagen alignment has been characterized by wavelet transform type

methods [18,19]. These techniques are rather expensive; they require specialized equipment and are restricted to specific subtypes of collagen fibers. In the clinical setting, trichrome staining is a common collagen staining approach. However, it is subject to high staining inconsistencies across institutions and even across different subjects from the same cohort. Furthermore, trichrome stains not only collagen, but also other undesired tissues [5,16,32].

Image Analysis and Machine Learning Methods: Hand-crafted ridge detectors have been used for several applications, such as for neurite in fluorescence microscopy images [22], for enhancement of vessel structures [29,12], and for detecting wrinkles on human skin [25]. Hidayat el. al. [14] have leveraged ridge detection for real-time texture boundary detection on natural images. There have been previous attempts to characterize structure of collagen from a machine learning perspective using hand-crafted features on spectroscopy images. Mayerich et. al. [21] have classified several types of tissues, including collagen, on a breast histology dataset of mid-infrared spectroscopy images. This method uses random forests and features from principal component analysis. [15,23] train a support vector machine (SVM) classifier using texture features from multi-photon microscopy images and second-harmonic generation microscopy images, respectively. The collagen fiber orientation in human arteries in light microscopic images was explored in [9]. Here, robust clustering and morphological operations in the color space were first used to identify fiber regions. This was followed by ridge and valley defections to calculate fiber orientations. Subsequently, region growing was used to obtain areas of homogenous fiber orientation. However, none of the previous works have utilized deep learning based methods to characterize fiber orientations. This is partly owing to the lack of well annotated pathology datasets. The ability of flow-based approaches to enhance image characteristics provides us the unique opportunity to leverage such methods in the context of our problem by fusing them with deep learning methods in a multi-stream setting.

Two-stream networks have been successfully applied in video analytics tasks, where spatial (frames) and temporal information (optical flow) are aggregated as shown in [30,26,10]. Particularly, [26] explores multiple fusion methods of intermediate outputs for human action recognition. Lin et al. [17] have introduced a new application of two-stream networks, where the architecture can model local pairwise feature interactions in a translationally invariant manner which is particularly useful for fine-grained categorization. Our methods leverage such two-stream networks in conjunction with gradient-based operators to build a curliness classifier on DUET images.

3 Methodology

We first introduce the filtering operations using the ridge filter. Next, we explain how to combine the ridge filter with deep neural networks in a seamless fashion in order to train a robust collagen fiber classifier.

3.1 Ridge Filter for Collagen fiber Structure Detection

Hessian-based filters are well-suited for detection of curvelinear structures in various biomedical contexts, such as vessels [12], neurons [22], etc. In particular, we employ a ridge detector. In a 2D image, ridges are the collection of curves on which the function value remains almost constant along the tangent direction, and are local maxima along the normal direction. See Fig. 2 for sample input DUET patches and the ridge detection results. The ridge detector successfully highlights the fiber structures so that they can be used to distinguish curly vs. straight patterns.

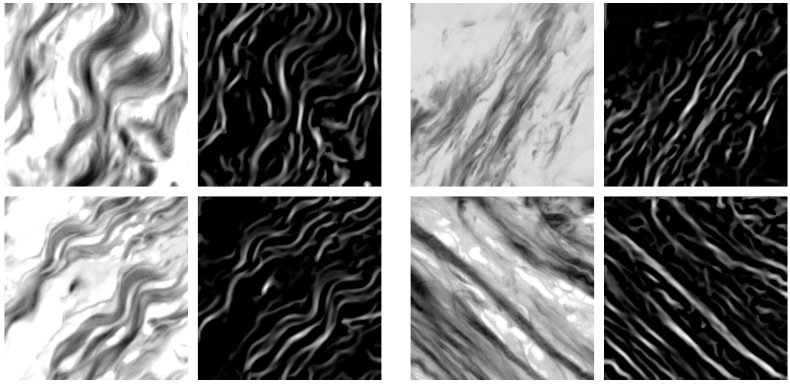

Fig. 2. A ridge detector is applied to curly and straight patches. From left to right: the DUET patches of curly structures, their corresponding ridge filter response, the DUET patches of straight structures, their ridge filter responses. Note the original image is inverted before the ridge filer being applied.

A ridge detector relies on the Hessian matrix of a gray-scale image. At any point of the image domain, the eigenvalues and eigenvectors of the Hessian correspond to the two principle curvatures and their corresponding directions (called principle directions). On a point in a ridge, one of the two Hessian eigenvalues will be close to zero (curvature along the tangent direction), the other will be negative (curvature along the normal direction). Ridge detectors identify ridge points based on this principle. Our method is particularly inspired by the one by Meijering et al. [22].

Our algorithm for ridge detection is illustrated in Fig. 3. At first, the original DUET image (A) is inverted so that the white pixels correspond to collagen fibre. Next, the image is smoothed with a Gaussian filter to ensure numerical stability when computing the second-degree derivatives (B). Next, the Hessian matrix $\mathcal{H}$ is calculated for each pixel in the smoothed image (denoted as $\mathcal{I}$) as follows

$$\mathcal{H}_{i,j} = \frac{\partial^2 \mathcal{I}}{\partial x_i \partial x_j} \tag{1}$$

where x_i and x_j are the two dimensions of the image domain. Since the Hessian matrix is symmetric, its eigenvalues can be computed as

$$\lambda_1 = \frac{1}{2}\left[\mathcal{H}_{1,1} + \mathcal{H}_{2,2} + (\sqrt{4\mathcal{H}_{1,2}^2 + (\mathcal{H}_{1,1} - \mathcal{H}_{2,2})^2})\right], \tag{2}$$

$$\lambda_2 = \frac{1}{2}\left[\mathcal{H}_{1,1} + \mathcal{H}_{2,2} - (\sqrt{4\mathcal{H}_{1,2}^2 + (\mathcal{H}_{1,1} - \mathcal{H}_{2,2})^2})\right]. \tag{3}$$

We rank the two eigenvalues based on their absolute magnitudes. We call λ_L and λ_H the low and high eigenvalues with respect to the absolute magnitude, or in short, the *low* and *high* eigenvalues. For each pixel, we have

$$\lambda_L = \text{argmin}_{\lambda \in \{\lambda_1, \lambda_2\}} |\lambda| \tag{4}$$

$$\lambda_H = \text{argmax}_{\lambda \in \{\lambda_1, \lambda_2\}} |\lambda| \tag{5}$$

Figures C.1 and C.2 visualize the low and high eigenvalues respectively. We note that the high eigenvalues can be either positive and negative. The desired ridge points are the locations whose λ_H has high absolute magnitude yet negative sign. To achieve this goal, we normalize λ_H by setting dividing it by the global minimal λ_H. This way, the range of the results can be up to +1. Figure D shows the results. As we can see, the ridge points have values close to 1. They correspond to points whose λ_H has high absolute magnitude yet negative sign. Finally, we remove irrelevant responses by setting all negative values to zero. See Figure E for the final filter response.

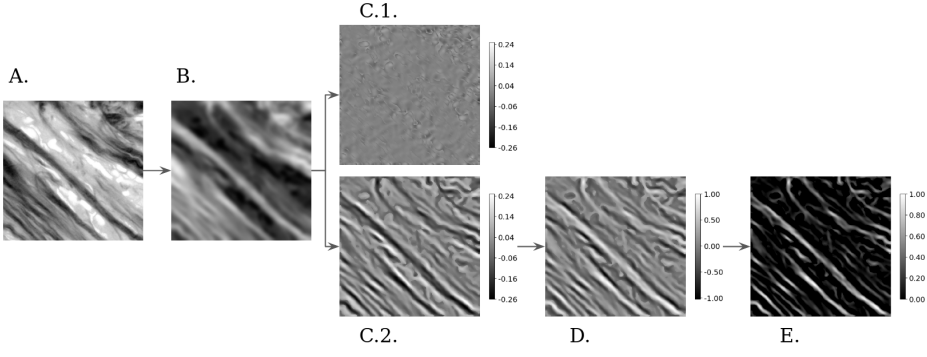

Fig. 3. A. Raw input patch. B. Input is inverted and smoothed with a Gaussian filter. C.1 Low eigenvalues λ_L of Equation 4. C.2 High eigenvalues λ_H of Equation 5. D. High eigenvalues λ_H are divided by its minimum value. E. Final ridge detection results after the negative values of the previous step are set to zero.

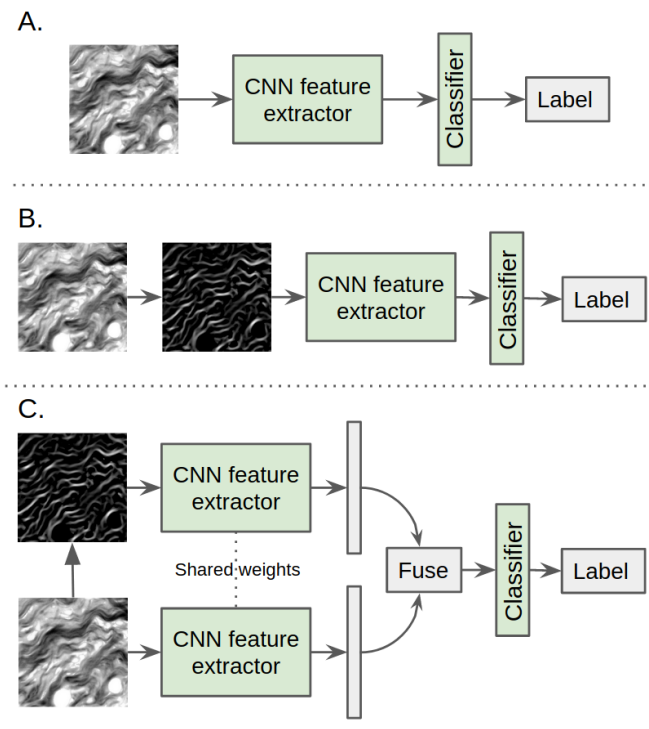

Fig. 4. A. The input is the raw patch of collagen content. B. The ridge detector is applied to the raw patch before feeding into the CNN. C. Features of the raw patch and the ridge detector response are fused for the classification.

3.2 Convolutional Neural Networks

We explore 3 different settings of training CNNs with ridge filter response as shown in Fig. 4. All experiments use ResNet [13] models with pre-trained weights using ImageNet. The backbone network has frozen weights and its output is an 1D-vector of size 512. In the first setting, the input to the CNN are the original DUET patches. We apply transfer learning by fine-tuning the final layers for two classes (curly and straight). In the second setting, the ridge detector is applied to the original DUET patches and is then provided to the CNN for transferred learning. In the third setting, the original DUET patch and the ridge filter are both use as input for a pretrained network. The output of the network are high-level feature representations of the original image and the ridge response. We fuse these features for the final binary classifier training.

We investigate 4 types of feature fusion strategies. Element-wise product (Elt-wise prod) is the element-wise multiplication of the elements of two 1D input vectors and its output has the same size. Similarly, Addition outputs a 1D vector of same size as the inputs and its elements are the sum of the elements of the two 1D input vectors. Another method is the concatenation of both 1D input vectors. Finally, we use the bilinear operation for two-stream networks, introduced in [17]. It computes the L2-normalized outer product of the two features as the input feature for the final classifier.

4 Experiments

Dataset and Settings. Six whole slide images (WSIs) of DUET images of BCa tissue are used to evaluate the proposed method. Our study comprised images from aggressive early stage breast cancer patients with known 5-year distant metastasis status. For each WSI, our domain expert selected regions of interests (ROIs) with strong collagen structures (see the left part of Fig. 1). Preliminary binary labels are also given to these ROIs (as curly or straight). Next, non-overlapping patches were sampled from inside these ROIs. The size of the patches is 400×400 pixels with a physical resolution of 0.22 microns per pixel.

Each of these extracted patches are annotated by the domain annotator as curly, straight, mixed, and insufficient signal. We discard patches of mixed type or insufficient signal. The remaining ones are used for training and validation. 5 WSIs and 1 WSI were used to create the training set and validation set, respectively. The distribution of the patches is shown in Table 1.

The ResNet-family networks were trained using the Adam optimizer for 100 epochs with a learning rate of 0.001. Input patches were resized to 224×224 pixels. We followed standard data augmentation regimes such as a 0.5 probability of horizontally and vertically flipping as well as random rotation of the input by up to 20 degrees. For the ridge detection step, we use a σ value of 5 as smoothing factor in the Gaussian filter before computing the Hessian matrix.

Table 1. Distribution of 400 × 400 patches

	Training	Validation
Curly	1037	314
Straight	1018	418

Quantitative Results. For our binary classification problem, we evaluated the area under the ROC Curve (AUC). We compare the 3 pipelines of Fig. 4 and the results are presented in Table 2. We observe that when the networks were trained with the output of the ridge detector, they achieve higher AUC than when the networks were trained directly on raw patches. Furthermore, we explore 4 different methods to aggregate the outputs of as shown in part C. of Fig. 4. In this setting, the addition of the outputs of the CNN is the only method that can boost the AUC performance on most of the networks.

Although the feature fusion methods do not seem to achieve significantly higher accuracy, we suspect it is due to the insufficient training data. When scaling up to a larger cohort, we expect the feature fusion network will achieve higher accuracy and become the best choice in practice.

Table 2. Results (AUC) after fine-tuning the ResNet models using raw patch only, ridge response only, and feature fusion result. The latter case has 4 ways of combining the intermediate outputs of the CNN.

Network	Raw	Ridge	Raw + Ridge			
		$\sigma = 5$	Elt-wise prod	Bilinear	Concatenation	Addition
ResNet-18	0.7365	**0.8467**	0.7027	0.7545	0.8055	0.8148
ResNet-34	0.7415	0.8235	0.8321	0.8100	0.8129	**0.8423**
ResNet-50	0.7400	0.8352	0.8391	0.7582	0.8446	**0.8624**
ResNet-101	0.7774	0.8432	0.7677	0.7988	0.8199	**0.8463**
Average	0.7489	0.8372	0.7854	0.7804	0.8207	**0.8415**

Table 3 shows how the smoothing factor (σ) of the ridge filter affects the AUC performance of the ResNet models that were fine-tuned on patches with a ridge filter applied before feeding into the network as shown in part B. of Fig. 4. On average, the ResNet networks benefit the most when σ was 5, so we used this value for our experiments.

Qualitative results. The network with highest AUC from the previous section is used to predict the degree of curliness as a heatmap on the annotated regions of interest. We run inference on the non-overlapping patches from inside the regions of interest and we save the output of the softmax layer for the "curly" class. On the left side of Fig. 5, preliminary annotations of the regions of interest

Table 3. Results (AUC) of the fine-tuned ResNet models when the input of the CNN is the output of the ridge detector. σ is the smoothing factor of the ridge detector.

	Ridge Filter			
Network	$\sigma = 1$	$\sigma = 3$	$\sigma = 5$	$\sigma = 7$
ResNet-18	0.6968	0.8151	**0.8467**	0.8402
ResNet-34	0.7202	0.7934	**0.8235**	0.8231
ResNet-50	0.7589	0.8289	0.8352	**0.8354**
ResNet-101	0.7383	0.8179	**0.8432**	0.8203
Average	0.7286	0.8138	**0.8372**	0.8298

are depicted for a WSI. The red boundary regions correspond to areas with dominating curliness and the blue boundary regions are dominantly straight. The predicted heatmap is shown on the right side of Fig. 5 and each pixel represents the likelihood of curliness of a patch of 400×400 pixels. We observe high consistency between patchwise prediction of our model and the preliminary labels of ROIs. On the bottom of Fig. 5, we also included a magnification of a sub-region of the WSI.

5 Conclusion

In an effort to optimize the research and clinical opportunities of tumor associated collagen as a predictive and prognostic biomarker, it is imperative to first localize the collagen content and then characterize the degree of curliness to further elucidate the relationship of collagen structure with tumor progression and metastasis. We present a quantitative approach that identifies characteristic collagen architecture in a unique dataset of BCa DUET images. Rather than learning to estimate collagen patterns using standard deep learning approaches directly on the DUET images, we enhance the images using ridge detectors and incorporate the filter responses using a feature-fusion strategy. Our work provides a novel and promising direction for research in digital pathology that can both further our understanding of BCa biology and meaningfully impact clinical management. Our results show that certain primitives can be enhanced in the pre-analytical steps, which can then help in providing additional architectural information about tissue samples. This can then be further integrated with other types of digital pathology analyses like automated tumor and TIL detection and characterization of different immunohistochemical (IHC) stains.

References

1. Brabrand, A., Kariuki, I.I., Engstrøm, M.J., Haugen, O.A., Dyrnes, L.A., Åsvold, B.O., Lilledahl, M.B., Bofin, A.M.: Alterations in collagen fibre patterns in breast cancer. a premise for tumour invasiveness? Apmis **123**(1), 1–8 (2015)

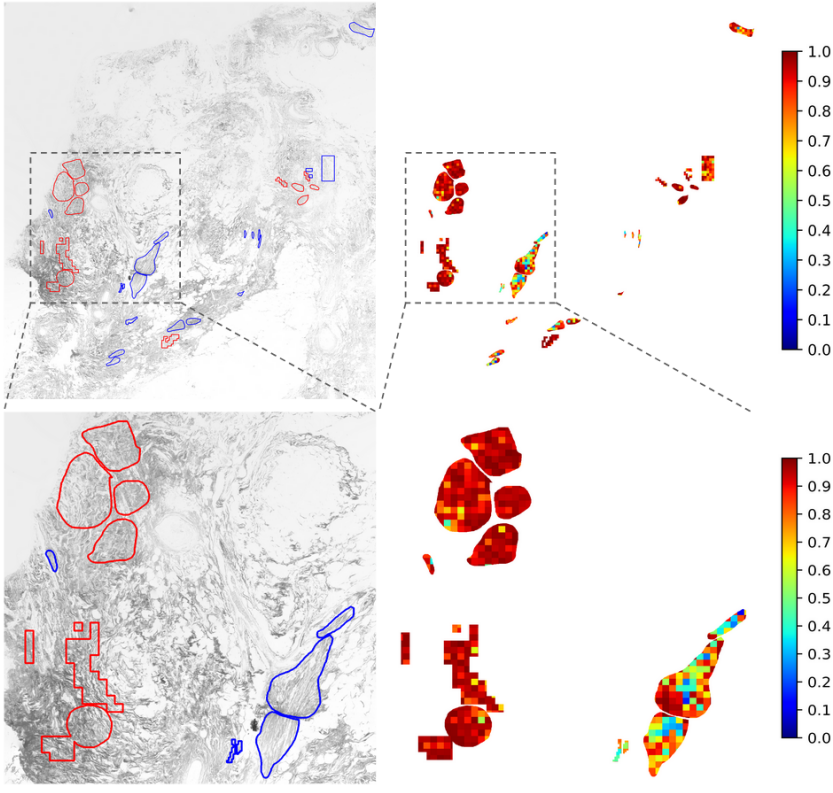

Fig. 5. Visualization of prediction results of our method. A high value on the heatmap represents a high likelihood of curliness. Left: ROIs on a WSI. Colors of the boundaries correspond to preliminary annotation by our experts. Red boundaries enclose regions that are dominantly curly. Blue boundaries enclose dominantly straight regions. Right: The likelihood map of curliness predicted by our method. Top: Full size WSI. Bottom: Magnification of a sub-region.

2. Burke, K., Tang, P., Brown, E.: Second harmonic generation reveals matrix alterations during breast tumor progression. Journal of biomedical optics **18**(3), 031106–031106 (2013)
3. Carpino, G., Overi, D., Melandro, F., Grimaldi, A., Cardinale, V., Di Matteo, S., Mennini, G., Rossi, M., Alvaro, D., Barnaba, V., et al.: Matrisome analysis of intrahepatic cholangiocarcinoma unveils a peculiar cancer-associated extracellular matrix structure. Clinical proteomics **16**(1), 1–12 (2019)
4. Case, A., Brisson, B.K., Durham, A.C., Rosen, S., Monslow, J., Buza, E., Salah, P., Gillem, J., Ruthel, G., Veluvolu, S., et al.: Identification of prognostic collagen signatures and potential therapeutic stromal targets in canine mammary gland carcinoma. PLOS one **12**(7), e0180448 (2017)
5. Cason, J.E.: A rapid one-step mallory-heidenhain stain for connective tissue. Stain Technology **25**(4), 225–226 (1950)
6. Cavaco, A.C.M., Dâmaso, S., Casimiro, S., Costa, L.: Collagen biology making inroads into prognosis and treatment of cancer progression and metastasis. in vivo **17**, 19 (2020)
7. Dolber, P., Spach, M.: Conventional and confocal fluorescence microscopy of collagen fibers in the heart. Journal of Histochemistry and Cytochemistry **41**(3), 465–469 (1993)
8. Drifka, C.R., Loeffler, A.G., Mathewson, K., Keikhosravi, A., Eickhoff, J.C., Liu, Y., Weber, S.M., Kao, W.J., Eliceiri, K.W.: Highly aligned stromal collagen is a negative prognostic factor following pancreatic ductal adenocarcinoma resection. Oncotarget **7** (2016)
9. Elbischger, P., Bischof, H., Regitnig, P., Holzapfel, G.: Automatic analysis of collagen fiber orientation in the outermost layer of human arteries. Pattern analysis and applications **7**(3), 269–284 (2004)
10. Feichtenhofer, C., Pinz, A., Zisserman, A.: Convolutional two-stream network fusion for video action recognition. In: Proceedings of the IEEE conference on computer vision and pattern recognition. pp. 1933–1941 (2016)
11. Fereidouni, F., Todd, A., Li, Y., Chang, C.W., Luong, K., Rosenberg, A., Lee, Y.J., Chan, J.W., Borowsky, A., Matsukuma, K., et al.: Dual-mode emission and transmission microscopy for virtual histochemistry using hematoxylin-and eosin-stained tissue sections. Biomedical Optics Express **10**(12), 6516–6530 (2019)
12. Frangi, A.F., Niessen, W.J., Vincken, K.L., Viergever, M.A.: Multiscale vessel enhancement filtering. In: International conference on medical image computing and computer-assisted intervention. pp. 130–137. Springer (1998)
13. He, K., Zhang, X., Ren, S., Sun, J.: Deep residual learning for image recognition. In: Proceedings of the IEEE conference on computer vision and pattern recognition. pp. 770–778 (2016)
14. Hidayat, R., Green, R.D.: Real-time texture boundary detection from ridges in the standard deviation space. In: BMVC. pp. 1–10 (2009)
15. Kistenev, Y.V., Vrazhnov, D.A., Nikolaev, V.V., Sandykova, E.A., Krivova, N.A.: Analysis of collagen spatial structure using multiphoton microscopy and machine learning methods. Biochemistry (Moscow) **84**(1), 108–123 (2019)
16. Lillie, R., Miller, G.: Histochemical acylation of hydroxyl and amino groups. effect on the periodic acid schiff reaction, anionic and cationic dye and van gieson collagen stains. Journal of Histochemistry & Cytochemistry **12**(11), 821–841 (1964)
17. Lin, T.Y., RoyChowdhury, A., Maji, S.: Bilinear cnn models for fine-grained visual recognition. In: Proceedings of the IEEE international conference on computer vision. pp. 1449–1457 (2015)

18. Liu, Y., Keikhosravi, A., Mehta, G.S., Drifka, C.R., Eliceiri, K.W.: Methods for quantifying fibrillar collagen alignment. In: Fibrosis, pp. 429–451. Springer (2017)
19. Liu, Y., Keikhosravi, A., Pehlke, C.A., Bredfeldt, J.S., Dutson, M., Liu, H., Mehta, G.S., Claus, R., Patel, A.J., Conklin, M.W., et al.: Fibrillar collagen quantification with curvelet transform based computational methods. Frontiers in Bioengineering and Biotechnology **8**, 198 (2020)
20. Majeed, H., Okoro, C., Kajdacsy-Balla, A., Toussaint, K.C., Popescu, G.: Quantifying collagen fiber orientation in breast cancer using quantitative phase imaging. Journal of biomedical optics **22**(4), 046004 (2017)
21. Mayerich, D.M., Walsh, M., Kadjacsy-Balla, A., Mittal, S., Bhargava, R.: Breast histopathology using random decision forests-based classification of infrared spectroscopic imaging data. In: Medical Imaging 2014: Digital Pathology. vol. 9041, p. 904107. International Society for Optics and Photonics (2014)
22. Meijering, E., Jacob, M., Sarria, J.C., Steiner, P., Hirling, H., Unser, M.: Design and validation of a tool for neurite tracing and analysis in fluorescence microscopy images. Cytometry Part A: the journal of the International Society for Analytical Cytology **58**(2), 167–176 (2004)
23. Mostaço-Guidolin, L.B., Ko, A.C.T., Wang, F., Xiang, B., Hewko, M., Tian, G., Major, A., Shiomi, M., Sowa, M.G.: Collagen morphology and texture analysis: from statistics to classification. Scientific reports **3**(1), 1–10 (2013)
24. Natal, R.A., Vassallo, J., Paiva, G.R., Pelegati, V.B., Barbosa, G.O., Mendonça, G.R., Bondarik, C., Derchain, S.F., Carvalho, H.F., Lima, C.S.: Collagen analysis by second-harmonic generation microscopy predicts outcome of luminal breast cancer. Tumor Biol. **40**(4) (2018)
25. Ng, C.C., Yap, M.H., Costen, N., Li, B.: Automatic wrinkle detection using hybrid hessian filter. In: Asian Conference on Computer Vision. pp. 609–622. Springer (2014)
26. Park, E., Han, X., Berg, T.L., Berg, A.C.: Combining multiple sources of knowledge in deep cnns for action recognition. In: 2016 IEEE Winter Conference on Applications of Computer Vision (WACV). pp. 1–8. IEEE (2016)
27. Provenzano, P.P., Eliceiri, K.W., Campbell, J.M., Inman, D.R., White, J.G., Keely, P.J.: Collagen reorganization at the tumor-stromal interface facilitates local invasion. BMC medicine **4**(1), 1–15 (2006)
28. Provenzano, P.P., Inman, D.R., Eliceiri, K.W., Knittel, J.G., Yan, L., Rueden, C.T., White, J.G., Keely, P.J.: Collagen density promotes mammary tumor initiation and progression. BMC medicine **6**(1), 1–15 (2008)
29. Sato, Y., Nakajima, S., Shiraga, N., Atsumi, H., Yoshida, S., Koller, T., Gerig, G., Kikinis, R.: Three-dimensional multi-scale line filter for segmentation and visualization of curvilinear structures in medical images. Medical image analysis **2**(2), 143–168 (1998)
30. Simonyan, K., Zisserman, A.: Two-stream convolutional networks for action recognition in videos. In: Advances in neural information processing systems. pp. 568–576 (2014)
31. Velez, D., Tsui, B., Goshia, T., Chute, C., Han, A., Carter, H., Fraley, S.: 3d collagen architecture induces a conserved migratory and transcriptional response linked to vasculogenic mimicry. Nature communications **8**(1), 1–12 (2017)
32. Whittaker, P., Kloner, R., Boughner, D., Pickering, J.: Quantitative assessment of myocardial collagen with picrosirius red staining and circularly polarized light. Basic research in cardiology **89**(5), 397–410 (1994)